

The 95 GeV Excess in the Georgi-Machacek Model: Single or Twin Peak Resonance

Amine Ahriche ^{1,*}

¹*Department of Applied Physics and Astronomy,
University of Sharjah, P.O. Box 27272 Sharjah, UAE.*

In this work, we investigate the possibility to address the excess observed around 95 GeV in the $\gamma\gamma$, $\tau\tau$, and $b\bar{b}$ channels as a scalar resonance(s) within the Georgi-Machacek (GM) model. In our analysis, we find that the excess can be easily accommodated in the channels ($\gamma\gamma$ and $b\bar{b}$) simultaneously, where the 95 GeV candidate is a single peak resonance (SPR) due to a light CP-even scalar. We found that the excess in the $\tau\tau$ channel can be addressed simultaneously with $\gamma\gamma$ and $b\bar{b}$ only if the 95 GeV candidate is a twin peak resonance (TPR), i.e., another CP-odd scalar in addition to the CP-even scalar. We demonstrate that the nature of the 95 GeV scalar resonance candidate (SPR or TPR) can be probed via the properties of its di- τ decay.

I. INTRODUCTION

Since the Higgs boson discovery with a mass around 125 GeV [1], the question about how the electroweak symmetry breaking (EWSB) proceeded, remains open. It is not clear yet whether the EWSB proceeded via a single Higgs as in the standard model (SM) or via many scalars as in many SM extensions. Therefore, the LHC physics program is devoting many searches and analyses to the search for a di-Higgs signal and the search for additional scalar resonances, whether they are heavier or lighter than the 125 GeV Higgs, for example see [2, 3].

Although many searches for light scalar (η) have been performed at LEP and the LHC (8+13 TeV), where an excess around 95 GeV has been reported in the channels [4–7]

$$\begin{aligned}\mu_{\gamma\gamma}^{\text{exp}} &= \mu_{\gamma\gamma}^{\text{ATLAS+CMS}} = \frac{\sigma^{\text{exp}}(gg \rightarrow \eta \rightarrow \gamma\gamma)}{\sigma^{\text{SM}}(gg \rightarrow h \rightarrow \gamma\gamma)} = 0.27_{-0.09}^{+0.10}, \\ \mu_{\tau\tau}^{\text{exp}} &= \mu_{\tau\tau}^{\text{CMS}} = \frac{\sigma^{\text{exp}}(gg \rightarrow \eta \rightarrow \tau\tau)}{\sigma^{\text{SM}}(gg \rightarrow h \rightarrow \tau\tau)} = 1.2 \pm 0.5, \\ \mu_{bb}^{\text{exp}} &= \mu_{bb}^{\text{LEP}} = \frac{\sigma^{\text{exp}}(e^+e^- \rightarrow Z\eta \rightarrow Zb\bar{b})}{\sigma^{\text{SM}}(e^+e^- \rightarrow Zh \rightarrow Zb\bar{b})} = 0.117 \pm 0.057,\end{aligned}\quad (1)$$

with local significance values 3.2σ [8], 2.2σ [4] and 2.3σ [9], respectively.

Regarding the significant difference between the observed values in (1), addressing the excess in the three channels simultaneously via a single particle is a very difficult, see, for example [10–43]. From model building point of view, in order to explain the excess in the different channels (1) as a scalar resonance, the 95 GeV scalar candidate should have SM-like couplings. In many new physics (NP) models, the 95 GeV scalar resonance candidate exhibits couplings to both gauge bosons and fermions that scale similarly with respect to the SM values, i.e., $\frac{g_{\eta ff}^{\text{NP}}}{g_{\eta VV}^{\text{NP}}} \sim \frac{g_{h ff}^{\text{SM}}}{g_{h VV}^{\text{SM}}}$. A NP model can successfully address the excess in these channels simultaneously if the couplings of the 95 GeV scalar resonance candidate to the SM fermions and gauge bosons are uncorrelated, i.e., $\frac{g_{\eta ff}^{\text{NP}}}{g_{\eta VV}^{\text{NP}}} \neq \frac{g_{h ff}^{\text{SM}}}{g_{h VV}^{\text{SM}}}$. This feature does exist in the so-called Georgi-Machacek (GM) model [44], where it has been shown that a viable parameter space exists for the light CP-even scalar case

*Electronic address: ahriche@sharjah.ac.ae

(η) with SM-like couplings [45]. Many phenomenological aspects of this model have been extensively studied in the literature [46–72].

The GM scalar sector has a residual global custodial $SU(2)_V$ symmetry after the EWSB, where its spectrum consists of two CP-even singlets (h and η), a triplet (H_3^0, H_3^\pm) and a quintuplet ($H_5^0, H_5^\pm, H_5^{\pm\pm}$). In this study, we explore whether the 95 GeV scalar resonance candidate could be the CP-even scalar single peak resonance (SPR) η (with a mass around 95 GeV), or a twin peak resonance (TPR) consisting of both the CP-even η and CP-odd H_3^0 , each with a degenerate mass around $m_\eta \approx m_{H_3^0} \sim 95$ GeV. A viable parameter space can be defined by confronting these two possibilities with the relevant theoretical and experimental constraints.

This work is organized as follows; in Section II, we review the GM model where we define the mass spectrum and the relevant scalar couplings. Then, in Section III, we discuss the different theoretical and experimental constraints relevant to our study. We discuss the 95 GeV signal excess in the $\gamma\gamma$, $\tau\tau$ and $b\bar{b}$ channels within the GM model in Section IV; where the relevant parameter space is identified. In Section V, we discuss the possibility of distinguishing the SPR and TPR scenarios using the di- τ channel. In Section VI, we give our conclusion.

II. MODEL, MASS SPECTRUM & COUPLINGS

In the GM model, the scalar sector consists of a doublet $(\phi^+, \phi^0)^T$; a complex triplet $(\chi^{++}, \chi^+, \chi^0)^T$ and a real triplet $(\xi^+, \xi^0, -\xi^-)^T$ with the hypercharge $Y = 1, 2, 0$, respectively;

$$\Phi = \begin{pmatrix} \frac{h_\phi - ia_\phi}{\sqrt{2}} & \phi^+ \\ -\phi^- & \frac{h_\phi + ia_\phi}{\sqrt{2}} \end{pmatrix}, \Delta = \begin{pmatrix} \frac{h_\chi - ia_\chi}{\sqrt{2}} & \xi^+ & \chi^{++} \\ -\chi^- & h_\xi & \chi^+ \\ \chi^{--} & -\xi^- & \frac{h_\chi + ia_\chi}{\sqrt{2}} \end{pmatrix}, \quad (2)$$

where the tree-level custodial symmetry is ensured by the scalar vacuum expectation values (VEVs) choice $\{\langle h_\phi \rangle, \langle h_\chi \rangle, \langle h_\xi \rangle\} = \{v_\phi, \sqrt{2}v_\xi, v_\xi\}$ with $v_\phi^2 + 8v_\xi^2 \equiv v_{SM}^2$. The GM scalar potential is invariant under the global symmetry $SU(2)_L \times SU(2)_R \times U(1)_Y$; and given by

$$V(\Phi, \Delta) = \frac{m_1^2}{2} \text{Tr}[\Phi^\dagger \Phi] + \frac{m_2^2}{2} \text{Tr}[\Delta^\dagger \Delta] + \lambda_1 (\text{Tr}[\Phi^\dagger \Phi])^2 + \lambda_2 \text{Tr}[\Phi^\dagger \Phi] \text{Tr}[\Delta^\dagger \Delta] + \lambda_3 \text{Tr}[(\Delta^\dagger \Delta)^2] + \lambda_4 (\text{Tr}[\Delta^\dagger \Delta])^2 - \lambda_5 \text{Tr}[\Phi^\dagger \frac{\sigma^a}{2} \Phi \frac{\sigma^b}{2}] \text{Tr}[\Delta^\dagger T^a \Delta T^b] - \mu_1 \text{Tr}[\Phi^\dagger \frac{\sigma^a}{2} \Phi \frac{\sigma^b}{2}] (U \Delta U^\dagger)_{ab} - \mu_2 \text{Tr}[\Delta^\dagger T^a \Delta T^b] (U \Delta U^\dagger)_{ab}, \quad (3)$$

where $\sigma^{1,2,3}$ are the Pauli matrices and $T^{1,2,3}$ correspond to the generators of the $SU(2)$ triplet representation and the matrix U is given in [44]. The GM scalar potential (3) is invariant under the global symmetry $SU(2)_L \times SU(2)_R \times U(1)_Y$ that is broken to a residual $SU(2)_V$ during the EWSB. The scalar spectrum includes three CP-even eigenstates $\{h_\phi, h_\chi, h_\xi\} \rightarrow \{h, \eta, H_5^0\}$, a neutral Goldstone and CP-odd eigenstate $\{a_\phi, a_\chi\} \rightarrow \{G^0, H_3^0\}$, a charged Goldstone and two singly charged scalars $\{\phi^\pm, \chi^\pm, \xi^\pm\} \rightarrow \{G^\pm, H_3^\pm, H_5^\pm\}$, and one doubly charged scalar $\chi^{\pm\pm} \equiv H_5^{\pm\pm}$, that are defined as [44]

$$h = c_\alpha h_\phi - \frac{s_\alpha}{\sqrt{3}} (\sqrt{2}h_\chi + h_\xi), \eta = s_\alpha h_\phi + \frac{c_\alpha}{\sqrt{3}} (\sqrt{2}h_\chi + h_\xi), H_5^0 = \sqrt{\frac{2}{3}} h_\xi - \sqrt{\frac{1}{3}} h_\chi, \\ H_3^0 = -s_\beta a_\phi + c_\beta a_\chi, H_3^\pm = -s_\beta \phi^\pm + c_\beta \frac{1}{\sqrt{2}} (\chi^\pm + \xi^\pm), H_5^\pm = \frac{1}{\sqrt{2}} (\chi^\pm - \xi^\pm), H_5^{\pm\pm} = \chi^{\pm\pm}, \quad (4)$$

with $s_x = \sin x$, $c_x = \cos x$ ($x = \alpha, \beta$); and $t_\beta \equiv \tan \beta = \sqrt{8}v_\xi/v_\phi$ and $\tan 2\alpha = 2M_{12}^2/(M_{22}^2 - M_{11}^2)$, where M^2 is the scalar squared mass matrix in the basis $\{h_\phi, \sqrt{\frac{2}{3}}h_\chi + \frac{1}{\sqrt{3}}h_\xi\}$. One has to mention that the CP-even scalar $H_5^0 = \sqrt{\frac{2}{3}}h_\xi - \frac{1}{\sqrt{3}}h_\chi$ does not couple to the SM fermions, and therefore cannot play any role in explaining this anomaly.

In this setup, the CP-odd scalar H_3^0 couples to the SM fermions but not to both gauge bosons, however, the CP-even scalar η (95 GeV candidate) has SM-like couplings to the gauge fields and fermions. Let us define the $SX\bar{X}$ coupling modifiers with respect to the SM in the GM model with $S = h, \eta, H_3^0$ and $X = \mu, \tau, b, c, W, Z, \gamma, \tilde{g}$. Lets us call $\varrho_X = \frac{g_{SX\bar{X}}^{GM}}{g_{hX\bar{X}}^{SM}}$ for $\varrho_X = \kappa_X, \zeta_X, \vartheta_X$, i.e.,

$$\begin{aligned}\kappa_F &= \frac{g_{hff}^{GM}}{g_{hff}^{SM}} = \frac{c_\alpha}{c_\beta}, \quad \kappa_V = \frac{g_{hVV}^{GM}}{g_{hVV}^{SM}} = c_\alpha c_\beta - \sqrt{\frac{8}{3}} s_\alpha s_\beta, \\ \zeta_F &= \frac{g_{\eta FF}^{GM}}{g_{hFF}^{SM}} = \frac{s_\alpha}{c_\beta}, \quad \zeta_V = \frac{g_{\eta VV}^{GM}}{g_{hVV}^{SM}} = s_\alpha c_\beta + \sqrt{\frac{8}{3}} c_\alpha s_\beta, \\ \vartheta_F &= \frac{g_{H_3^0 FF}^{GM}}{g_{hFF}^{SM}} = -s_\alpha, \quad \vartheta_V = \frac{g_{H_3^0 VV}^{GM}}{g_{hVV}^{SM}} = 0.\end{aligned}\quad (5)$$

Here, we have $F = \mu, \tau, b, c$ and $V = W, Z$. The scalar gluon effective vertices are mediated by the top/bottom quark loops, which implies $\varrho_{\tilde{g}} = \varrho_F$, while the scalar photon effective coupling modifiers are given by

$$\varrho_\gamma = \left| \frac{\varrho_V A_1^{\gamma\gamma} (4m_W^2/m_S^2) + \varrho_F \frac{4}{3} A_{1/2}^{\gamma\gamma} (4m_t^2/m_S^2) + \varrho_F \frac{1}{3} A_{1/2}^{\gamma\gamma} (4m_b^2/m_S^2) + \frac{v}{2} \sum_i \frac{g_{SX\bar{X}}^{GM}}{m_X^2} Q_X^2 A_0^{\gamma\gamma} (4m_X^2/m_S^2)}{A_1^{\gamma\gamma} (4m_W^2/m_S^2) + \frac{4}{3} A_{1/2}^{\gamma\gamma} (4m_t^2/m_S^2) + \frac{1}{3} A_{1/2}^{\gamma\gamma} (4m_b^2/m_S^2)} \right|, \quad (6)$$

where $X = H_3^\pm, H_5^\pm, H_5^{\pm\pm}$ stands for all charged scalars inside the loop diagrams, Q_X is the electric charge of the field X in units of $|e|$, $g_{SX\bar{X}}^{GM}$ are triple couplings of the scalar $S = h, \eta, H_3^0$ to the charged scalars, respectively; and the one-loop functions $A_i^{\gamma\gamma}$ are given in [73].

One has to mention that in the GM model, there exists an invariance under the transformation $(v_\xi, \mu_{1,2}) \rightarrow (-v_\xi, -\mu_{1,2})$, which means $V(\Phi, \Delta, \mu_{1,2}) = V(\Phi, -\Delta, -\mu_{1,2})$. The scalar mass matrix elements also remain invariant under this transformation. However, because the physical scalar eigenstates are mixtures of the components of the doublet and triplets, most of the physical triple and quartic scalar vertices are not invariant under $(v_\xi, \mu_{1,2}) \rightarrow (-v_\xi, -\mu_{1,2})$. This implies that any two benchmark points (BPs) with the same input parameters but with different signs of $(\pm t_\beta, \pm \mu_{1,2})$ are physically different. This can be easily seen in the couplings modifier (5); thus, negative t_β values should not be ignored in the numerical scan.

III. THEORETICAL & EXPERIMENTAL CONSTRAINTS

In our analysis, we consider many theoretical and experimental constraints such as tree-level unitarity, boundness from below, Higgs measurements (total decay width and coupling modifiers); and different negative searches at LEP and the LHC. These constraints are detailed in [45, 71]. It has been shown that the GM scalar potential may acquire some minima that violate the CP symmetry or the electric charge, that are deeper than the electroweak vacuum $\{v_\phi, \sqrt{2}v_\xi, v_\xi\}$. This fact excludes about 40% of the parameter space that is usually considered in the literature [71].

Since the scalar resonance candidates η and H_3^0 mass is around 95 GeV, their decay is mainly to $\mu\mu, \tau\tau, bb, cc, \gamma\gamma, \tilde{g}\tilde{g}$. For the Higgs and the 95 GeV scalar resonance candidates $S = h, \eta, H_3^0$, one writes

$$\Gamma_S^{tot} = \Gamma_S^{SM} \sum_{X=SM} \varrho_X^2 \mathcal{B}^{SM}(S \rightarrow XX), \quad \mathcal{B}(S \rightarrow XX) = \varrho_X^2 \left(\Gamma_S / \Gamma_S^{SM} \right)^{-1}, \quad (7)$$

where the SM numerical values of Γ_S^{SM} and $\mathcal{B}^{SM}(S \rightarrow XX)$ are given in [74]. This allows the partial signal strength modifier at the LHC for the scalar S to be simplified within the Narrow Width Approximation

(NWA) as

$$\begin{aligned}\mu_{XX}^S &= \frac{\sigma(pp \rightarrow S) \times \mathcal{B}(S \rightarrow XX)}{\sigma^{SM}(pp \rightarrow h) \times \mathcal{B}^{SM}(h \rightarrow XX)} \\ &= \kappa_F^2 \varrho_X^2 \left(\Gamma_S / \Gamma_S^{SM} \right)^{-1},\end{aligned}\quad (8)$$

where Γ_S and Γ_S^{SM} are the scalar total decay width and its SM values, i.e., $\Gamma_S^{SM} = \Gamma_h^{SM}(m_h \rightarrow m_S)$. One has to mention that in this setup, the channels $h \rightarrow \eta\eta, H_3H_3, H_5H_5$ and $\eta \rightarrow WW, ZZ, H_3H_3, H_5H_5$ ($H_3^0 \rightarrow WW, H_5H_5$) are kinematically forbidden due to $m_\eta \sim 95$ GeV ($m_{H_3^0} \sim 95$ GeV).

Here, we consider experimental measurements of the Higgs total decay width ($\Gamma_h = 4.6_{-2.5}^{+2.6}$ MeV [75]), the electroweak precision tests; and the Higgs strength signal modifiers μ_{XX}^h for $X = \mu, \tau, b, \gamma, W, Z$ [75]. One has to mention that the Higgs strength modifiers μ_{XX}^h for $X = \mu, \tau, b, W, Z$ can be obtained from (8) by replacing ϱ_X by κ_X in (5), while for $\mu_{\gamma\gamma}^h$, ϱ_X should be replaced by κ_γ in (6). In order to ensure simultaneous matching for all previous observables, we define a χ^2 function

$$\chi_{SM}^2 = \sum_{\mathcal{O}=1}^8 \chi_{\mathcal{O}}^2 = \sum_{\mathcal{O}=1}^8 \left(\frac{\mathcal{O} - \mathcal{O}^{\text{exp}}}{\Delta \mathcal{O}^{\text{exp}}} \right)^2, \quad (9)$$

where the observables \mathcal{O} denote (1) the Higgs total decay width (Γ_h), the Higgs signal strength modifiers (from 2 to 7) (μ_{XX}^h for $X = \mu, \tau, b, \gamma, W, Z$) and (8) the oblique parameter ΔS . One notices that the contribution of $\mu_{\gamma\gamma}^h$ to (9) is more important than those of $\mu_{\mu, \tau, \tau, bb, WW, ZZ}^h$ since it depends on the charged scalar masses and scalar couplings in addition to the mixing angles α and β [71]. In our analysis, we consider a precision of 95% C.L., i.e., $\chi_{SM}^2 < 12.59$ for eight variables. The experimental values of the oblique parameter in (9) are $S = 0.06 \pm 0.10$ [75]. One has to mention that the oblique parameter S was estimated in [61], while the oblique parameter T cannot be estimated in the GM model since the hypercharge interactions break the $SU(2)_R$ global symmetry at one-loop level, yielding a divergent value for the T parameter [55, 76].

Besides the above-mentioned constraints, others should be considered like the negative searches for doubly-charged Higgs bosons in the VBF channel $H_5^{++} \rightarrow W^+W^+$; and the Drell-Yan production of a neutral Higgs boson $pp \rightarrow H_5^0(\gamma\gamma)H_5^+$; which gives strong bounds on the parameter space [70]. It has been shown in [70], that the doubly-charged Higgs bosons in the VBF channel leads to important constraints from CMS on $s_\beta^2 \times \mathcal{B}(H_5^{++} \rightarrow W^+W^+)$ [77]. The negative search of the quintet in the di-photon channel $H_5^0 \rightarrow \gamma\gamma$ is translated into bounds on the fiducial cross section times branching ratio $\sigma_{fid} = (\sigma_{H_5^0 H_5^+} \times \epsilon_+ + \sigma_{H_5^0 H_5^-} \times \epsilon_-) \mathcal{B}(H_5^0 \rightarrow \gamma\gamma)$, which is constrained by ATLAS at 8 TeV [78] and at 13 TeV [79]. To incorporate these constraints into our numerical analysis, we utilized the formulas for the decay rate and the cross section, as well as the efficiency values used in [70]. Regarding the bounds from the null results in searches for $H_5^{++} \rightarrow W^+W^+$, the CMS analysis [77] only considered masses of $m_5 > 200$, GeV. Therefore, we extrapolated the existing bounds down to $m_5 > 78$, GeV.

At LEP, the negative searches for SM-like light scalars at low mass range $m_\eta < 100$ GeV impose a significant bound on the cross section of $e^-e^+ \rightarrow \eta Z$ [80], i.e., the factor ζ_V^2 . However, one notices that this bound is easily satisfied for the mass values around 95.4 GeV [45]. Another search of the light SM-like scalar in the di-photon channel with masses in the range 70 – 110 GeV has been performed by CMS at 8 TeV and 13 TeV [81], where upper bounds are established on the production cross section $\sigma(pp \rightarrow \eta) \times \mathcal{B}(\eta \rightarrow \gamma\gamma)$ scaled by its SM value, i.e., the factor $\zeta_F^2 \cdot \zeta_\gamma^2$, where ζ_X 's are defined in (5) and (6). Concerning the CMS bounds [81] on the production cross section of the CP-odd scalar $\sigma(pp \rightarrow H_3^0) \times \mathcal{B}(H_3^0 \rightarrow \gamma\gamma)$, the bounds are automatically fulfilled since $|\vartheta_F \cdot \vartheta_\gamma| < |\zeta_F \cdot \zeta_\gamma|$ for all the viable parameter space.

Since the charged triplet H_3^\pm is partially coming from the SM doublet as shown in (4), it then couples the up to the down quark in a similar way that the W gauge boson does. These interactions lead to flavor violating processes such as the $b \rightarrow s$ transition ones, which depend only on the charged triplet mass m_3

and the mixing angle β . The current experimental value of the $b \rightarrow s\gamma$ branching ratio, for a photon energy $E_\gamma > 1.6$ GeV is $\mathcal{B}(\overline{B} \rightarrow X_s\gamma)_{exp} = (3.55 \pm 0.24 \pm 0.09) \times 10^{-4}$, while the two SM predictions are $\mathcal{B}(\overline{B} \rightarrow X_s\gamma)_{SM} = (3.15 \pm 0.23) \times 10^{-4}$ [82] and $\mathcal{B}(\overline{B} \rightarrow X_s\gamma)_{SM} = (2.98 \pm 0.26) \times 10^{-4}$ [83]. In our numerical scan, we will consider the severe among the bounds on the m_3 - v_χ plan shown in Fig. 1 in [61].

IV. THE EXCESS IN THE $\gamma\gamma$, $\tau\tau$ AND $b\bar{b}$ CHANNELS

Here, we estimate the excess observed by both LEP and LHC around the 95.4 GeV mass value in the channels $\gamma\gamma$, $\tau\tau$, $b\bar{b}$, where the signal resonance is assumed to be a CP-even scalar for $93 \text{ GeV} < m_\eta < 97 \text{ GeV}$; or a superposition of two resonances if $93 \text{ GeV} < m_\eta, m_{H_3^0} < 97 \text{ GeV}$. Then, the 95 GeV signal resonance signal strength modifiers can be written in the NWA as

$$\begin{aligned}\mu_{\gamma\gamma}^{(95)} &= \mu_{\gamma\gamma}^{(\eta)} + \mu_{\gamma\gamma}^{(H_3^0)} \\ &= \zeta_F^2 \zeta_\gamma^2 \left(\Gamma_\eta / \Gamma_\eta^{SM} \right)^{-1} + \vartheta_F^2 \vartheta_\gamma^2 \left(\Gamma_{H_3^0} / \Gamma_{H_3^0}^{SM} \right)^{-1}, \\ \mu_{\tau\tau}^{(95)} &= \mu_{\tau\tau}^{(\eta)} + \mu_{\tau\tau}^{(H_3^0)} \\ &= \zeta_F^4 \left(\Gamma_\eta / \Gamma_\eta^{SM} \right)^{-1} + \vartheta_F^4 \left(\Gamma_{H_3^0} / \Gamma_{H_3^0}^{SM} \right)^{-1}, \\ \mu_{b\bar{b}}^{(95)} &= \mu_{b\bar{b}}^{(\eta)} = \zeta_V^2 \zeta_F^2 \left(\Gamma_\eta / \Gamma_\eta^{SM} \right)^{-1}.\end{aligned}\tag{10}$$

One remarks that the signal $\mu_{b\bar{b}}^{(95)}$ does not include the contribution $\mu_{b\bar{b}}^{(H_3^0)}$ since the CP-odd scalar H_3^0 does not couple to the Z gauge boson. Clearly, the CP-even scalar H_3^0 cannot play a similar role as H_3^0 since it does not couple to quarks and therefore cannot be ggF produced at the LHC; and it also does not decay into the SM fermions if produced at LEP.

In order to estimate the relative contributions $\rho_{\gamma\gamma, \tau\tau} = \mu_{\gamma\gamma, \tau\tau}^{(H_3^0)} / \mu_{\gamma\gamma, \tau\tau}^{(95)}$ in (10), one has to mention that because the H_3^0 total decay width is much smaller than its corresponding SM value, then the factor $(\Gamma_{H_3^0} / \Gamma_{H_3^0}^{SM})^{-1}$ may lead to a significant enhancement for $\mu_{\gamma\gamma, \tau\tau}^{(95)}$. In addition, the effective coupling modifier ϑ_γ is very suppressed due to the absence of the gauge and scalar contributions to ϑ_γ in (6). This makes the ratio $\rho_{\tau\tau} = \mu_{\tau\tau}^{(H_3^0)} / \mu_{\tau\tau}^{(95)}$ comparable to unity; but $\rho_{\gamma\gamma} = \mu_{\gamma\gamma}^{(H_3^0)} / \mu_{\gamma\gamma}^{(95)}$ is very suppressed, as will be shown next.

By considering all the above mentioned constraints discussed in Section III, we perform a numerical scan, where the masses lie in the ranges $93 \text{ GeV} < m_\eta < 97 \text{ GeV}$ and $78 \text{ GeV} < m_3, m_5 < 2 \text{ TeV}$, where $m_{3,5}$ are the triplet and quintuplet masses, respectively. The triplet mass ranges $93 \text{ GeV} < m_3 < 97 \text{ GeV}$ correspond to the TPR case; while the rest of the m_3 values correspond to the SPR scenario. In addition, we impose the SM-like Higgs constraints to be fulfilled at 95% C.L. by taking $\chi_{SM}^2 < 12.59$, where χ_{SM}^2 is defined in (9).

Concerning the 95 GeV signal excess (1), one defines the functions $\chi_{(N)}^2$ as

$$\chi_{(2)}^2 = \chi_{\gamma\gamma}^2 + \chi_{b\bar{b}}^2, \quad \chi_{(3)}^2 = \chi_{\gamma\gamma}^2 + \chi_{b\bar{b}}^2 + \chi_{\tau\tau}^2, \quad \chi_i^2 = \left(\frac{\mu_i - \mu_i^{\text{exp}}}{\Delta\mu_i^{\text{exp}}} \right)^2,\tag{11}$$

which are useful to check for whether the excess can be addressed simultaneously in the channels $\gamma\gamma$, $b\bar{b}$ and/or $\gamma\gamma$, $\tau\tau$, $b\bar{b}$, respectively. In our analysis, we will consider only the BPs that address the three channels simultaneously within $2 - \sigma$, i.e., $\chi_{(3)}^2 < 8.02$. In Fig. 1, we show the signal strength modifier values (10) and the $\chi_{(2)}^2$ ($\chi_{(3)}^2$) function for the considered BPs in the SPR (TPR) scenario in the up (bottom) panels.

From the upper panels in Fig. 1, one remarks that the excess in the channels $\gamma\gamma$ and $b\bar{b}$ is easily matched simultaneously in the SPR case, where the matching could be exact for some BPs as $\chi_{(2)}^2 \sim 10^{-6}$. According

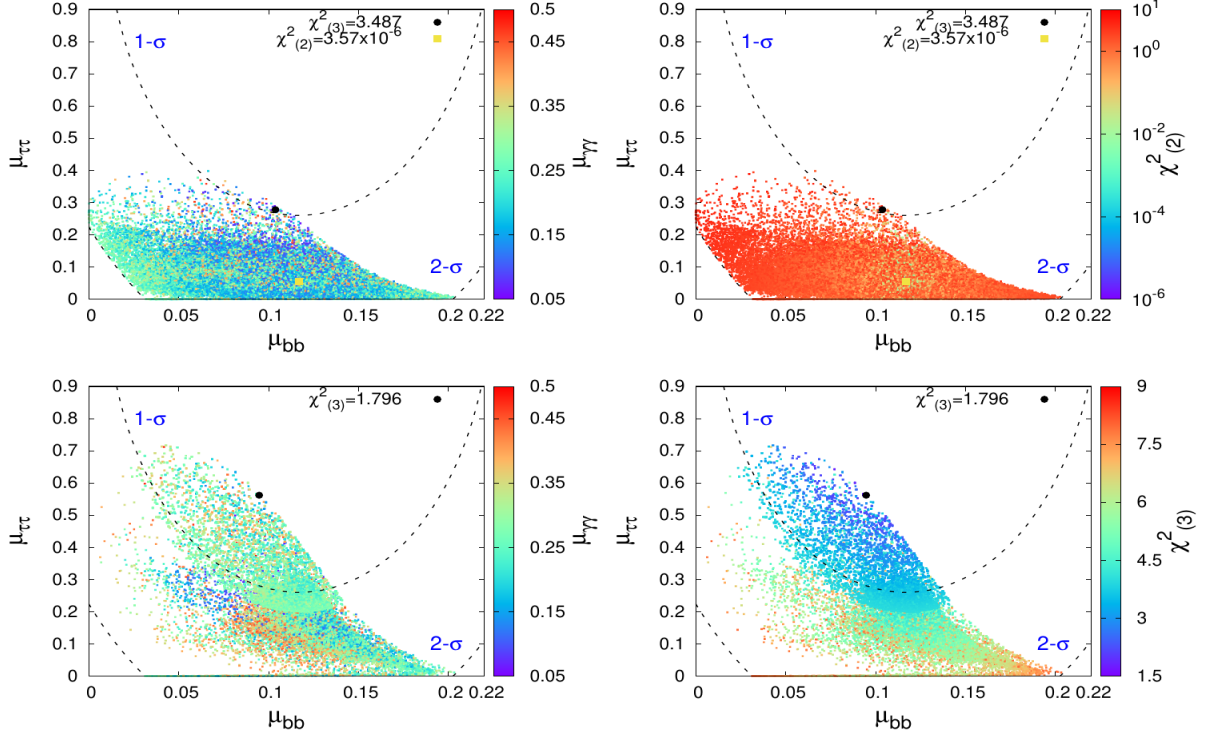


FIG. 1: The signal strength values (10) for 2σ viable BPs with $\chi^2_{(3)} < 8.02$, $\chi^2_{SM} < 12.59$ in the cases of SPR (top) and TPR (bottom). The black point represents the best fit BPs that corresponds to $BP_1 : \chi^2_{(3)} = 3.487$ and $BP_2 : \chi^2_{(3)} = 1.796$ for the SPR (top) and TPR cases, respectively. The yellow point in the upper panels represents the best matching of the excess in the channels $\gamma\gamma$ and $b\bar{b}$ ($BP_3 : \chi^2_{(2)} \sim 10^{-6}$). In the right panels, the $\chi^2_{(2)}$ ($\chi^2_{(3)}$) function (11) is shown in the upper (lower) palette.

to the minimal value $\chi^2_{(3)} = 3.487$, the excess could be addressed in the three channels $\gamma\gamma, b\bar{b}$ and $\tau\tau$ simultaneously in $1 - \sigma$ for tiny part of the parameter space (0.0059 % among all BPs) that corresponds to $\chi^2_{(3)} < 3.53$. This tiny region of the parameter space exists due to the large value of $\Delta\mu_{\tau\tau}^{\text{exp}} = 0.5$, so this region could be ruled out once precise measurements are performed for $\mu_{\tau\tau}$ despite the new central value. According to the bottom panels, the H_0^3 contribution to the signal strengths is very important to address the di- τ excess in the TPS case. Here, the $\chi^2_{(3)}$ values are getting significantly smaller than the SPR case. In the TPR case, we have about 27.5% of the BPs with less than $1 - \sigma$, which means that the excess in the three channels (1) is addressed simultaneously in the three channels. Whereas, in the SPR case, the $\chi^2_{(3)}$ function values are larger than $1 - \sigma$ for the majority of the BPs considered in Fig. 1, as its minimal value is $\chi^2_{(3)}^{\text{min}} = 3.487$. The best fit benchmark points BP_1, BP_2 and BP_3 shown in Fig. 1 are presented in Table I.

For reasons of completeness, we show the couplings modifiers ζ_X for the $1 - \sigma$ BPs in the SPR ($\chi^2_{(2)} < 2.3$) and TPR ($\chi^2_{(3)} < 3.53$) cases in Fig. 2.

From Fig. 2-right, it is clear that addressing this excess in the three channels simultaneously makes the parameter space for the TPR case so tight. However, if the di- τ excess would be relaxed to a smaller value like $\mu_{\tau\tau}^{(95)} \sim 0.6$ with a good precision $\Delta\mu_{\tau\tau}^{\text{exp}} \lesssim 0.1$ in future analyses, a significant part of the GM parameter space can address the three measurements simultaneously within both SPR scenario, while for the TPR scenario, we could get an exact matching, i.e., $\chi^2_{(3)} \sim 0$.

In some attempts to address the excess (1), it is believed that one of them can be regarded as statistical fluctuations, and hence, should disappear once more data are collected, for example see [84]. If the signal strength $\mu_{\tau\tau}^{(95)}$ will be relaxed to a smaller value once ATLAS results are reported and/or more data are

| | BP_1 | BP_2 | BP_3 |
|-----------------------------|--------|--------|----------------------|
| s_β | -0.511 | -0.496 | 0.345 |
| s_α | 0.488 | 0.458 | -0.220 |
| m_3 | 94.74 | 103.99 | 100.96 |
| m_5 | 78.15 | 79.38 | 121.62 |
| κ_F | 1.015 | 1.024 | 1.040 |
| κ_V | 0.903 | 0.911 | 0.962 |
| κ_γ | 1.027 | 0.931 | 0.956 |
| ζ_F | 0.568 | 0.528 | -0.235 |
| ζ_V | -0.308 | -0.322 | 0.344 |
| ζ_γ | 0.484 | 0.501 | 0.522 |
| ϑ_F | -0.489 | -0.458 | 0.220 |
| ϑ_γ | 0.149 | 0.140 | 0.067 |
| μ_1 | -51.31 | -55.48 | 41.42 |
| μ_2 | -29.69 | -22.17 | 67.95 |
| $\mu_{\gamma\gamma}^{(95)}$ | 0.257 | 0.251 | 0.270 |
| $\mu_{\tau\tau}^{(95)}$ | 0.562 | 0.278 | 0.054 |
| $\mu_{bb}^{(95)}$ | 0.095 | 0.104 | 0.117 |
| $\rho_{\tau\tau}$ | 0.575 | - | - |
| ΔS | -0.032 | -0.023 | -0.060 |
| $\chi_{(2)}^2$ | 0.168 | 0.088 | 3.7×10^{-6} |
| $\chi_{(3)}^2$ | 1.7959 | 3.4868 | 5.2493 |
| χ_{SM}^2 | 12.526 | 12.141 | 9.127 |

TABLE I: Different physical observables for the BPs shown in Fig. 1. All mass dimension observables are given in GeV.

considered by CMS, the excess in the three channels can be simultaneously addressed, even in the SPR case; and, hence the viable parameter space would be significant. In order to probe the H_0^3 contribution effect to (6) in the TPR case, we show the H_0^3 relative contributions to (6) in Fig. 3-left.

As expected, the H_0^3 contribution represents 14 ~ 58% of the signal strength $\mu_{\tau\tau}^{(95)}$, unlike its contribution to $\mu_{\gamma\gamma}^{(95)}$ that is practically vanishing. From Fig. 3, one mentions that large H_0^3 contributions to $\mu_{\tau\tau}^{(95)}$ are preferred, since they correspond to smaller values for $\chi_{(3)}^2 < 3.53$.

V. DISTINGUISHING THE SPR AND TPR SCENARIOS VIA THE DI- τ CHANNEL

If the 95 GeV excess is confirmed in the di- τ channel when new ATLAS results are reported using more data and/or similar results are released by CMS, this channel could be very useful for distinguishing between the SPR and TPR scenarios. In the SPR case, the CP properties of the 95 GeV signal resonance are well defined, matching those of a CP-even Higgs decaying into $\tau\tau$. However, in the TPR case, the CP properties would be different. Therefore, a mismatch of the CP-even properties in the $\tau\tau$ channel could confirm the TPR scenario.

At the detector level, the τ lepton cannot be measured directly but based on its decay products, especially the hadronic final states $\mathcal{B}(\tau \rightarrow had) = 64.79\%$ [75]. It has two important decay channels $\tau^\pm \rightarrow \pi^\pm \nu_\tau$ and $\tau^\pm \rightarrow \rho^\pm \nu_\tau \rightarrow \pi^\pm \pi^0 \nu_\tau$ with the branching ratios 10.82% and 25.49%, respectively. However, the decay $\eta(H_3^0) \rightarrow \tau^+ \tau^- \rightarrow \pi^+ \pi^- \nu_\tau \bar{\nu}_\tau$ is more useful to identify the scalar CP properties via the dependence on

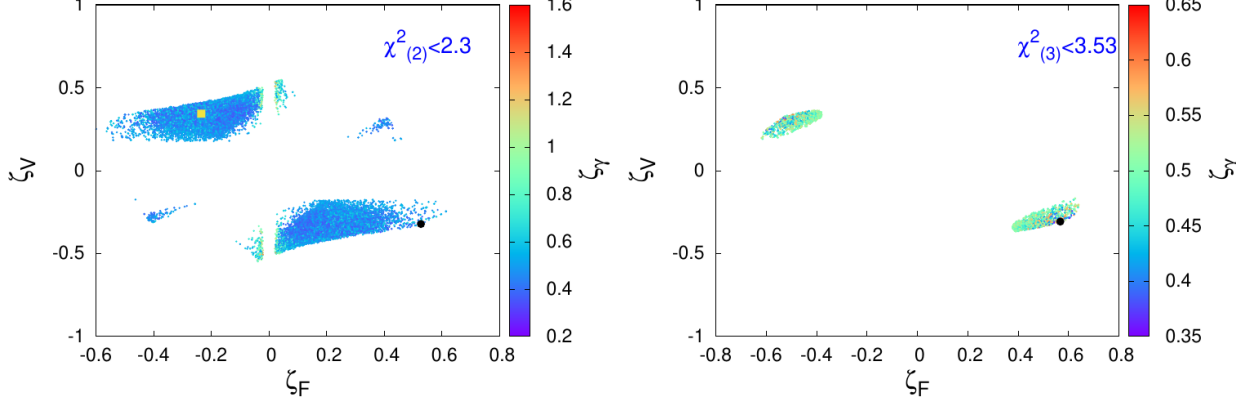


FIG. 2: The couplings modifiers ζ_X for the SPR (right) and TPR (left) cases. Here, we considered only the $1 - \sigma$ BPs, i.e., $\chi^2_{(2)} < 2.3$ ($\chi^2_{(3)} < 3.53$) for the SPR (TPR) case. The black points in the middle and right panels correspond to the BPs with $BP_1 : \chi^2_{(3)} = 3.487$ and $BP_2 : \chi^2_{(3)} = 1.796$, respectively, while the yellow one represents the BP with $BP_3 : \chi^2_{(2)} = 3.57 \times 10^{-6}$.

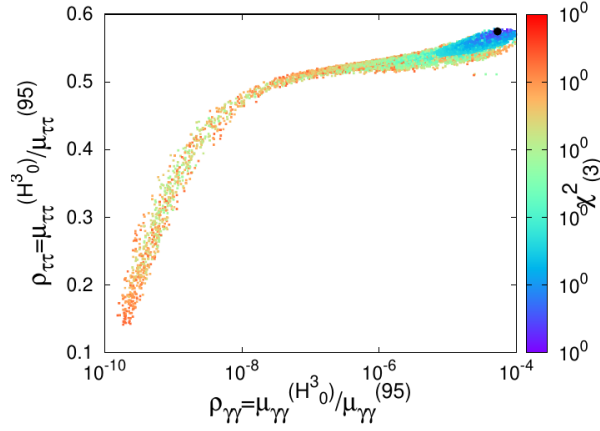


FIG. 3: The ratios $\mu_{\tau\tau}^{(H^0)}/\mu_{\tau\tau}^{(95)}$ and $\mu_{\gamma\gamma}^{(H^0)}/\mu_{\gamma\gamma}^{(95)}$ in the TPR case using the BPs considered in Fig. 1. Here, the palette represents the $\chi^2_{(3)}$ function.

the so-called acoplanarity angle that is defined as $\phi^* = \arccos(\vec{n}_+ \cdot \vec{n}_-)$, where \vec{n}_\pm are unit vectors that are normal to the decay plans of the charged pions. The ϕ^* distribution is generally used to probe the Higgs CP phase Δ_{CP} of the tau Yukawa interaction:

$$-\mathcal{L}_Y = y_\tau h \bar{\psi}_\tau (\cos(\Delta_{CP}) + i\gamma_5 \sin(\Delta_{CP})) \psi_\tau. \quad (12)$$

The acoplanarity angle normalized distributions for the cases of CP-even, CP-odd are given by

$$R_{even,odd}(\phi^*) = \frac{1}{N} \frac{dN}{d\phi^*} = \frac{1}{2\pi} [1 \mp Q \cos(\phi^*)], \quad (13)$$

with $Q = \frac{\pi^2}{16} \cdot \frac{\pi^2}{16} \left(\frac{m_\tau^2 - 2m_\rho^2}{m_\tau^2 + 2m_\rho^2} \right)^2$ for the decays $\tau \rightarrow \pi^- \nu_\tau$ and $\tau \rightarrow \rho^- \nu_\tau$, respectively [85]. While for a degenerate CP-even/CP-odd resonance, it is written by

$$R_{TPR}(\phi^*) = (1 - \rho_{\tau\tau}) R_{even}(\phi^*) + \rho_{\tau\tau} R_{odd}(\phi^*), \quad (14)$$

with $\rho_{\tau\tau} = \mu_{\tau\tau}^{(H^0)}/\mu_{\tau\tau}^{(95)}$ as presented previously in Fig. 3. Then, by considering the maximum/minimum values of the acoplanarity angle distribution (for example, $\phi^* = \pi$ if H_3^0 are pure CP-even and CP-odd

scalars, respectively), one obtains the ratio $\rho_{\tau\tau} = [1 + Q - 2\pi R_m]/[2Q]$, with R_m to be maximum/minimum of $R_{TPR}(\phi^*)$, which corresponds to $\phi^* = \pi$ for pure CP-even/CP-odd distribution. This can be easily confirmed numerically.

In Fig. 4, we show the normalized distribution of the acoplanarity angle (ϕ^*) in the final state $\tau^+\tau^- \rightarrow \pi^+\pi^-\nu_\tau\bar{\nu}_\tau$ for the SPR cases of CP conserving ($\Delta_{CP} = 0$) and CP violating ($\Delta_{CP} = \pi/4$) (magenta); and two TPR BPs with $\rho_{\tau\tau} = 0.1415$ (blue) and $\rho_{\tau\tau} = 0.57833$ (red).

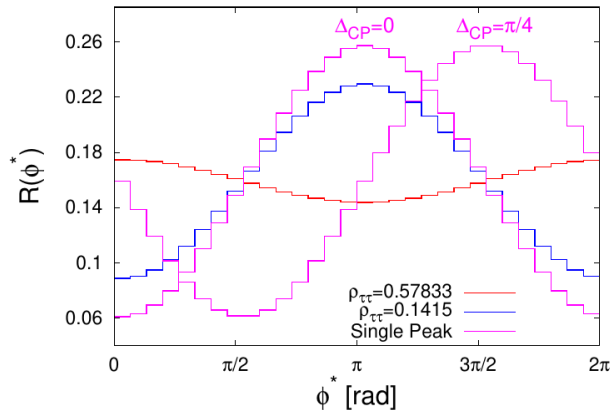


FIG. 4: The acoplanarity angle normalized distributions in the decay $\eta(H_3^0) \rightarrow \tau^+\tau^- \rightarrow \pi^+\pi^-\nu_\tau\bar{\nu}_\tau$ for two SPR cases ($\Delta_{CP} = 0, \pi/4$) in magenta color, and two TPR BPs with $\rho_{\tau\tau} = 0.1415$ (blue) and $\rho_{\tau\tau} = 0.57833$ (red).

One learns from Fig. 4 that the TPR case can be easily identified due to the flatness of the acoplanarity angle distribution; and can be distinguished from the case of a single resonance, whatever its CP phase value Δ_{CP} is for the tau Yukawa interaction in (12). In the case of a pure CP-even (CP-odd) scalar, i.e., $\Delta_{CP} = 0$ ($\Delta_{CP} = \pi/2$), the ϕ^* distribution has a maximum (minimum) at $\phi^* = \pi$ with same amplitude. So, obviously, if the contributions of η and H_3^0 are exactly equal, the distribution (14) would be a horizontal straight line. From Fig. 4, it is clear that the distribution values at $\phi^* = \pi$ for the red and blue curves lead to $\rho_{\tau\tau} = 0.1415$ and $\rho_{\tau\tau} = 0.57833$, respectively; according to the formula $\rho_{\tau\tau} = [1 + Q - 2\pi R_{TPR}(\phi^* = \pi)]/[2Q]$ mentioned previously.

VI. CONCLUSION

In this work, we have investigated the possibility of addressing the 95 GeV signal excess that is observed in the channels $\gamma\gamma, b\bar{b}$ and $\tau\tau$ within the GM model. We have found that this excess can be addressed in the GM model in two ways: (1) SPR case where the signal candidate is a CP-even scalar (η) with SM-like couplings; and (2) TPR case, where a CP-odd scalar (H_3^0) whose mass being around 95 GeV; contributes to this signal excess in addition to the CP-even scalar η . By imposing all relevant theoretical and experimental constraints on the model parameter space, the excess can be addressed in the channels $\gamma\gamma$ and $b\bar{b}$ simultaneously in the SPR case ($\chi_{(2)}^2 \sim 10^{-6}$). While in the TPR case, the three channels $\gamma\gamma, b\bar{b}$ and $\tau\tau$ can be addressed simultaneously ($1.796 \leq \chi_{(3)}^2 \leq 3.53$). This makes the parameter space tight, and the model more predictable at colliders since the Higgs couplings modifiers are lying in the ranges $0.90584 < \kappa_F < 1.0591$ and $0.89045 < \kappa_V < 0.99083$ for both SPR and TPR scenarios. Once the ATLAS di- τ excess will be reported and/or CMS analysis re-done using more data; and the di- τ excess may be relaxed to smaller value, let us say around $\mu_{\tau\tau}^{(95)} \sim 0.6$ with a good precision $\Delta\mu_{\tau\tau}^{\text{exp}} \lesssim 0.1$, then the GM model will be able to address the excess in the three channels simultaneous within both SPR and TPR scenarios.

We have shown also that the 95 GeV candidate scalar di- τ decay $\eta(H_3^0) \rightarrow \tau_h^+ \tau_h^-$ is very useful to identify whether it is a SPR or TPR case. The TPR case can be easily distinguished if the acoplanarity angle normalized distribution gets flattened with respect to the SPR case. For some specific values of the acoplanarity angle ($\phi^* = \pi$), one can estimate exactly the relative contributions of both CP-even and CP-odd to the 95 GeV signal resonance.

Acknowledgments: I would like to thank Salah Nasri for his useful comments on the manuscript. This work was funded by the University of Sharjah under the research projects No 21021430107 “*Hunting for New Physics at Colliders*” and No 23021430135 “*Terascale Physics: Colliders vs Cosmology*”.

-
- [1] G. Aad *et al.* [ATLAS], Phys. Lett. B **716** (2012), 1-29 [arXiv:1207.7214 [hep-ex]]. S. Chatrchyan *et al.* [CMS], Phys. Lett. B **716** (2012), 30-61 [arXiv:1207.7235 [hep-ex]]. I
- [2] G. Aad *et al.* [ATLAS], Eur. Phys. J. C **81** (2021) no.4, 332 [arXiv:2009.14791 [hep-ex]]. I
- [3] A. M. Sirunyan *et al.* [CMS], JHEP **09** (2018), 007 [arXiv:1803.06553 [hep-ex]]. I
- [4] [CMS], [arXiv:2208.02717 [hep-ex]]. I, I
- [5] C. Arcangeletti, *ATLAS, LHC Seminar*, indico.cern.ch/event/1281604, 2023.
- [6] A. Azatov, R. Contino and J. Galloway, JHEP **04** (2012), 127 [erratum: JHEP **04** (2013), 140] [arXiv:1202.3415 [hep-ph]].
- [7] J. Cao, X. Guo, Y. He, P. Wu and Y. Zhang, Phys. Rev. D **95** (2017) no.11, 116001 [arXiv:1612.08522 [hep-ph]]. I
- [8] T. Biekötter, S. Heinemeyer and G. Weiglein, Phys. Rev. D **109** (2024) no.3, 3 [arXiv:2306.03889 [hep-ph]]. I
- [9] R. Barate *et al.* [LEP Working Group for Higgs boson searches, ALEPH, DELPHI, L3 and OPAL], Phys. Lett. B **565** (2003), 61-75 [arXiv:hep-ex/0306033 [hep-ex]]. I
- [10] G. Cacciapaglia, A. Deandrea, S. Gascon-Shotkin, S. Le Corre, M. Lethuillier and J. Tao, JHEP **12** (2016), 068 [arXiv:1607.08653 [hep-ph]]. I
- [11] A. Crivellin, J. Heeck and D. Moeller, Phys. Rev. D **97** (2018) no.3, 035008 [arXiv:1710.04663 [hep-ph]].
- [12] J. Cao, X. Jia, Y. Yue, H. Zhou and P. Zhu, Phys. Rev. D **101** (2020) no.5, 055008 [arXiv:1908.07206 [hep-ph]].
- [13] T. Biekötter, M. Chakraborti and S. Heinemeyer, Eur. Phys. J. C **80** (2020) no.1, 2 [arXiv:1903.11661 [hep-ph]].
- [14] J. M. Cline and T. Toma, Phys. Rev. D **100** (2019) no.3, 035023 [arXiv:1906.02175 [hep-ph]].
- [15] A. A. Abdelalim, B. Das, S. Khalil and S. Moretti, Nucl. Phys. B **985** (2022), 116013 [arXiv:2012.04952 [hep-ph]].
- [16] S. Heinemeyer, C. Li, F. Lika, G. Moortgat-Pick and S. Paasch, Phys. Rev. D **106** (2022) no.7, 075003 [arXiv:2112.11958 [hep-ph]].
- [17] T. Biekötter, A. Grohsjean, S. Heinemeyer, C. Schwanenberger and G. Weiglein, Eur. Phys. J. C **82** (2022) no.2, 178 [arXiv:2109.01128 [hep-ph]].
- [18] T. Biekötter and M. O. Olea-Romacho, JHEP **10** (2021), 215 [arXiv:2108.10864 [hep-ph]].
- [19] W. Li, J. Zhu, K. Wang, S. Ma, P. Tian and H. Qiao, Chin. Phys. C **47** (2023) no.12, 123102 [arXiv:2212.11739 [hep-ph]].
- [20] T. Biekötter, S. Heinemeyer and G. Weiglein, Eur. Phys. J. C **83** (2023) no.5, 450 [arXiv:2204.05975 [hep-ph]].
- [21] R. Benbrik, M. Boukidi, S. Moretti and S. Semlali, PoS **ICHEP2022** (2022), 547 [arXiv:2211.11140 [hep-ph]].
- [22] S. Iguro, T. Kitahara and Y. Omura, Eur. Phys. J. C **82** (2022) no.11, 1053 [arXiv:2205.03187 [hep-ph]].
- [23] T. Biekötter, S. Heinemeyer and G. Weiglein, JHEP **08** (2022), 201 [arXiv:2203.13180 [hep-ph]].
- [24] R. Benbrik, M. Boukidi, S. Moretti and S. Semlali, Phys. Lett. B **832** (2022), 137245 [arXiv:2204.07470 [hep-ph]].
- [25] T. Biekötter, S. Heinemeyer and G. Weiglein, Phys. Lett. B **846** (2023), 138217 [arXiv:2303.12018 [hep-ph]].
- [26] D. Azevedo, T. Biekötter and P. M. Ferreira, JHEP **11** (2023), 017 [arXiv:2305.19716 [hep-ph]].
- [27] A. Ahriche, M. L. Bellilet, M. O. Khojali, M. Kumar and A. T. Mulaudzi, Phys. Rev. D **110** (2024) no.1, 015025 [arXiv:2311.08297 [hep-ph]].
- [28] T. K. Chen, C. W. Chiang, S. Heinemeyer and G. Weiglein, Phys. Rev. D **109** (2024) no.7, 075043

- [arXiv:2312.13239 [hep-ph]].
- [29] P. S. B. Dev, R. N. Mohapatra and Y. Zhang, Phys. Lett. B **849** (2024), 138481 [arXiv:2312.17733 [hep-ph]].
- [30] W. Li, H. Qiao, K. Wang and J. Zhu, [arXiv:2312.17599 [hep-ph]].
- [31] S. Bhattacharya, G. Coloretti, A. Crivellin, S. E. Dahbi, Y. Fang, M. Kumar and B. Mellado, [arXiv:2306.17209 [hep-ph]].
- [32] G. Coloretti, A. Crivellin, S. Bhattacharya and B. Mellado, Phys. Rev. D **108** (2023) no.3, 035026 [arXiv:2302.07276 [hep-ph]].
- [33] S. Ashanujjaman, S. Banik, G. Coloretti, A. Crivellin, B. Mellado and A. T. Mulaudzi, Phys. Rev. D **108** (2023) no.9, L091704 [arXiv:2306.15722 [hep-ph]].
- [34] C. X. Liu, Y. Zhou, X. Y. Zheng, J. Ma, T. F. Feng and H. B. Zhang, Phys. Rev. D **109** (2024) no.5, 056001 [arXiv:2402.00727 [hep-ph]].
- [35] J. Cao, X. Jia and J. Lian, [arXiv:2402.15847 [hep-ph]].
- [36] J. Kalinowski and W. Kotlarski, [arXiv:2403.08720 [hep-ph]].
- [37] U. Ellwanger and C. Hugonie, [arXiv:2403.16884 [hep-ph]].
- [38] G. Arcadi, G. Busoni, D. Cabo-Almeida and N. Krishnan, [arXiv:2311.14486 [hep-ph]].
- [39] A. Arhrib, K. H. Phan, V. Tran and T. C. Yuan, [arXiv:2405.03127 [hep-ph]].
- [40] R. Benbrik, M. Boukidi and S. Moretti, [arXiv:2405.02899 [hep-ph]].
- [41] S. Y. Ayazi, M. Hosseini, S. Paktinat Mehdiabadi and R. Rouzbehi, [arXiv:2405.01132 [hep-ph]].
- [42] U. Ellwanger, C. Hugonie, S. F. King and S. Moretti, [arXiv:2404.19338 [hep-ph]].
- [43] K. Wang and J. Zhu, [arXiv:2402.11232 [hep-ph]]. I
- [44] H. Georgi and M. Machacek, Nucl. Phys. B **262**, 463-477 (1985). I, II
- [45] A. Ahriche, Phys. Rev. D **107** (2023) no.1, 015006, Erratum Phys. Rev. D 108, 019902 (2023) [arXiv:2212.11579 [hep-ph]]. I, III, III
- [46] M. S. Chanowitz and M. Golden, Phys. Lett. B **165**, 105-108 (1985) I
- [47] J. F. Gunion, R. Vega and J. Wudka, Phys. Rev. D **42**, 1673-1691 (1990)
- [48] H. E. Haber and H. E. Logan, Phys. Rev. D **62**, 015011 (2000) [arXiv:hep-ph/9909335 [hep-ph]].
- [49] M. Aoki and S. Kanemura, Phys. Rev. D **77**, no.9, 095009 (2008) [erratum: Phys. Rev. D **89**, no.5, 059902 (2014)] [arXiv:0712.4053 [hep-ph]].
- [50] S. Godfrey and K. Moats, Phys. Rev. D **81**, 075026 (2010) [arXiv:1003.3033 [hep-ph]].
- [51] I. Low and J. Lykken, JHEP **10**, 053 (2010) [arXiv:1005.0872 [hep-ph]].
- [52] H. E. Logan and M. A. Roy, Rev. D **82**, 115011 (2010) [arXiv:1008.4869 [hep-ph]].
- [53] S. Chang, C. A. Newby, N. Raj and C. Wanotayaroj, Phys. Rev. D **86**, 095015 (2012) [arXiv:1207.0493 [hep-ph]].
- [54] S. Kanemura, M. Kikuchi and K. Yagyu, Phys. Rev. D **88**, 015020 (2013) [arXiv:1301.7303 [hep-ph]].
- [55] C. Englert, E. Re and M. Spannowsky, Rev. D **87**, no.9, 095014 (2013) [arXiv:1302.6505 [hep-ph]]. III
- [56] R. Killick, K. Kumar and H. E. Logan, 033015 (2013) [arXiv:1305.7236 [hep-ph]].
- [57] C. Englert, E. Re and M. Spannowsky, 035024 (2013) [arXiv:1306.6228 [hep-ph]].
- [58] N. Ghosh, S. Ghosh and I. Saha, Phys. Rev. D **101** (2020) no.1, 015029 [arXiv:1908.00396 [hep-ph]].
- [59] D. Das and I. Saha, Phys. Rev. D **98** (2018) no.9, 095010 [arXiv:1811.00979 [hep-ph]].
- [60] K. Hartling, K. Kumar and H. E. Logan, Phys. Rev. D **90** (2014) no.1, 015007 [arXiv:1404.2640 [hep-ph]].
- [61] K. Hartling, K. Kumar and H. E. Logan, Phys. Rev. D **91** (2015) no.1, 015013 [arXiv:1410.5538 [hep-ph]]. III
- [62] C. W. Chiang, S. Kanemura and K. Yagyu, Phys. Rev. D **90** (2014) no.11, 115025 [arXiv:1407.5053 [hep-ph]].
- [63] C. W. Chiang, S. Kanemura and K. Yagyu, Phys. Rev. D **93** (2016) no.5, 055002 [arXiv:1510.06297 [hep-ph]].
- [64] J. Chang, C. R. Chen and C. W. Chiang, JHEP **03** (2017), 137 [arXiv:1701.06291 [hep-ph]].
- [65] C. W. Chiang and K. Tsumura, JHEP **04** (2015), 113 [arXiv:1501.04257 [hep-ph]].
- [66] T. K. Chen, C. W. Chiang, C. T. Huang and B. Q. Lu, [arXiv:2205.02064 [hep-ph]].
- [67] S. L. Chen, A. Dutta Banik and Z. K. Liu, Nucl. Phys. B **966** (2021), 115394 [arXiv:2011.13551 [hep-ph]].
- [68] T. Pilkington, [arXiv:1711.04378 [hep-ph]].
- [69] C. W. Chiang and T. Yamada, Phys. Lett. B **735** (2014), 295-300 [arXiv:1404.5182 [hep-ph]].
- [70] A. Ismail, H. E. Logan and Y. Wu, [arXiv:2003.02272 [hep-ph]]. III
- [71] Z. Baire and A. Ahriche, Phys. Rev. D **108** (2023) no.5, 5 [arXiv:2207.00142 [hep-ph]]. III, III

- [72] S. Ghosh, [arXiv:2311.15405 [hep-ph]]. I
- [73] A. Djouadi, Phys. Rept. **457** (2008), 1-216 [arXiv:hep-ph/0503172 [hep-ph]]. II
- [74] The LHC Higgs Working Group: <https://twiki.cern.ch/twiki/bin/view/LHCPhysics/LHCHWG> III
- [75] R. L. Workman *et al.* [Particle Data Group], PTEP **2022** (2022), 083C01. III, III, V
- [76] J. F. Gunion, R. Vega and J. Wudka, Phys. Rev. D **43** (1991), 2322-2336. III
- [77] A. M. Sirunyan *et al.* [CMS], Phys. Rev. Lett. **120** (2018) no.8, 081801 [arXiv:1709.05822 [hep-ex]]. III
- [78] G. Aad *et al.* [ATLAS], Phys. Rev. Lett. **113** (2014) no.17, 171801 [arXiv:1407.6583 [hep-ex]]. III
- [79] M. Aaboud *et al.* [ATLAS], Phys. Lett. B **775** (2017), 105-125 [arXiv:1707.04147 [hep-ex]]. III
- [80] G. Abbiendi *et al.* [OPAL], Eur. Phys. J. C **27** (2003), 311-329 [arXiv:hep-ex/0206022 [hep-ex]]. III
- [81] A. M. Sirunyan *et al.* [CMS], Phys. Lett. B **793** (2019), 320-347 [arXiv:1811.08459 [hep-ex]]. III
- [82] M. Misiak, H. M. Asatrian, K. Bieri, M. Czakon, A. Czarnecki, T. Ewerth, A. Ferroglia, P. Gambino, M. Gorbahn and C. Greub, *et al.* Phys. Rev. Lett. **98** (2007), 022002 [arXiv:hep-ph/0609232 [hep-ph]]. III
- [83] T. Becher and M. Neubert, Phys. Rev. Lett. **98** (2007), 022003 [arXiv:hep-ph/0610067 [hep-ph]]. III
- [84] J. A. Aguilar-Saavedra, H. B. Camara, F. R. Joaquim and J. F. Seabra, Phys. Rev. D **108** (2023) no.7, 075020 [arXiv:2307.03768 [hep-ph]]. IV
- [85] J. H. Kuhn and F. Wagner, Nucl. Phys. B **236** (1984), 16-34 V